Optical Guiding of Atoms through a Hollow-Core Photonic Band-Gap Fiber

T. Takekoshi and R. J. Knize

Laser and Optics Research Center, Department of Physics, United States Air Force Academy, Colorado 80840, USA

(Received 11 December 2006; published 25 May 2007)

We demonstrate the first guiding of atoms through a hollow-core photonic band-gap fiber. Rb atoms from a thermal oven source travel through 6.1 and 4.0 cm long fibers with a guiding potential $1/e^2$ radius of 3.0 μm. When the photon scattering rate is small, the observed guiding efficiency is greater than 70%. An unexpected low-speed cutoff is attributed to inefficient optical coupling.

DOI: 10.1103/PhysRevLett.98.210404 PACS numbers: 39.25.+k, 03.75.Be, 42.70.Qs

Matter waveguides have been demonstrated using both magnetic [1–3] and optical potentials [4–7]. A waveguide capable of transverse confinement in a single vibrational state allows the possibility of monochromatic, single spatial-mode guided matter interferometry. This requires cold atoms and a tight, lossless potential. Previous optical guides use hollow glass capillary tubes and have atom losses due to multimode speckle patterns. Speckle can cause local loss of confinement, leading to wall collisions. Capillary guides also have light losses due to coupling with unguided modes. This limits their useful length. A recent development in photonic crystal technology known as the hollow-core photonic band-gap (HCPBG) fiber [8] is an ideal candidate for developing robust and compact atom interferometers because one can guide light in a single low-loss spatial mode (several micrometers in diameter) at bending radii of a few centimeters. In theory, there is no speckle and long waveguides are possible. High power and large red detunings can be used to produce attractive potentials with low spontaneous emission. Atoms in these guides would also be ideal for studying low-light-level interactions [9]. In this Letter, we demonstrate a straight HCPBG fiber guide for Rb atoms.

The apparatus is shown in Fig. 1. The Rb source is an oven with a reservoir held at 100 °C. The oven chamber itself is slightly hotter ($T = 125$ °C) and features a large-aperture nozzle or collimator (0.2 cm diameter, 1.6 cm long) whose exit is 12.7 cm from the fiber entrance. The nozzle dimensions were chosen to be large enough to guarantee proper alignment while maintaining a reasonable reservoir lifetime. The calculated Rb mean free path inside the oven (0.8 cm) is on the order of the nozzle dimensions, so that the beam operates at the edge of the effusive regime. Because low-speed atoms do not appear at the detection chamber on the other end of the fiber, we had to verify that these atoms were not being depleted by intrabeam scattering. We confirmed their presence by measuring the fluorescence versus frequency caused by a probe laser beam at 68° to the atomic beam about halfway between the nozzle and the fiber [Fig. 1(a)]. The HCPBG fiber is held in a stainless steel capillary tube which is pressure fit into a hole drilled through a double-sided vacuum flange. This flange separates the source chamber from the detection chamber. The transmitted atom signal with no guiding light present is smaller than the detector dark noise limit of 0.4 ions/s. The signal with guiding light present due to background Rb vapor in the source chamber, as measured by blocking the oven, is small compared to the atomic beam signal.

The guiding light comes from a single-frequency Ti:sapphire laser. It is 10 to 350 GHz red-detuned from the ^{85}Rb $D1$ (795 nm) or $D2$ (780 nm) transition. When a single linearly polarized beam is coupled into the HCPBG fiber, the near-field intensity profile varies periodically with polarization and frequency [10]. Power shifts back and forth between two lobes inside the core. In the far field, the output polarization can vary considerably across the intensity profile. The birefringence changes with frequency and input polarization. This behavior is due to polarization-dependent coupling to surface modes [11] and varies in strength over the range of the photonic band gap, disappearing almost completely near 860 nm. Using two input beams with orthogonal polarizations results in a roughly Gaussian near-field profile which does not vary much (Fig. 2). The guiding light is transported to the HCPBG fiber coupling optics using a step index polarization-preserving fiber. Each beam is coupled to one polarization axis, and because of the acousto-optic modulator (AOM) they have slightly different frequencies (Fig. 1). The frequency difference (140 MHz) is negligible compared to the laser detuning, to the period over which the single-polarization mode profile changes, and to the free spectral range corresponding to the fiber length, but is much larger than the natural transverse oscillation frequency of the atom. A mirror in the source chamber can be moved into the atomic beam path to intercept light exiting the HCPBG fiber so that the transmitted power can be measured.

Guided atoms are detected by two-step ionization [Fig. 1(b)]. ^{85}Rb atoms emerging from the fiber pass through three collinear detection beams which are perpendicular to the fiber and tuned to $5S_{1/2}(F = 3) \rightarrow 5P_{3/2}(F = 4)$ (780 nm $D2$, pump), $5S_{1/2}(F = 2) \rightarrow 5P_{1/2}(F = 3)$ (795 nm $D1$, repump), and $5P_{3/2} \rightarrow$ continuum (458 nm, ionization). The resulting ions are collected by a Channeltron detector biased at -2050 V. Output pulses are recorded by a scaler. The AOM can be

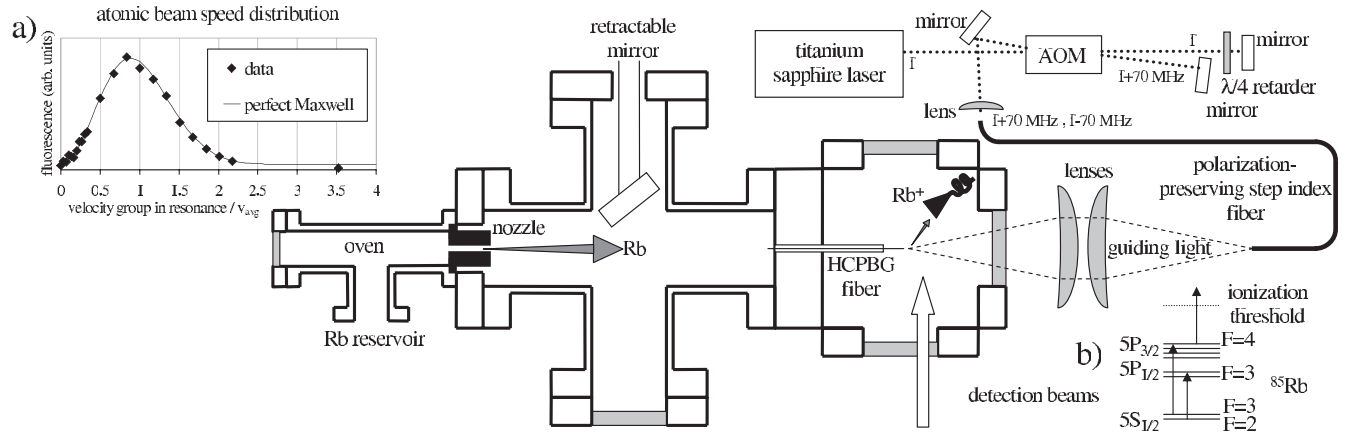

FIG. 1. Guiding apparatus. A double-passed 70 MHz acousto-optic modulator (AOM) allows two-beam guiding and switches the guiding light on and off for time-of-flight (TOF) spectroscopy. (a) Atomic beam fluorescence versus resonant speed, in units of $v_{avg} = \sqrt{8k_BT/\pi m}$. (b) ^{85}Rb is detected by two-step ionization.

used to switch the guiding light on suddenly so that a time-of-flight (TOF) spectrum can be observed (Fig. 3).

Because the kinetic energy of the atoms (~400 K) is much larger than the guiding potential depth (~0.1 K), guiding can only occur if an atom has sufficiently low transverse kinetic energy once it is inside the fiber. Trajectory simulations show that, for slower atoms, the throughput is limited by the solid angle subtended by the oven nozzle at the fiber entrance, while the effective capture area on the input face of the fiber (a circular area defining the maximum impact parameter for which guiding occurs) is independent of input angle and speed to within 20%. A high-speed cutoff in the speed distribution (a delayed onset of the TOF signal) is expected because the maximum guiding angle of incidence for fast atoms becomes very small. The low-speed cutoff seen in the data (sudden early termination of growth later in the TOF signal) is not expected. To investigate this, we measured the upper and lower cutoff speeds v_U and v_L for various powers and detunings of the guiding light by fitting the model indicated by the dark line in Fig. 3 to the TOF data. The cutoffs, in units of $v_{avg} = \sqrt{8k_BT/\pi m}$, for two different 6.1 cm long HCPBG fibers (Blaze Photonics models HC800-01 and HC800-02) are shown in Fig. 4. The −01 fiber has a slightly larger mode size (3.8 μm $1/e^2$ intensity radius) than the −02 fiber (3.0 μm) as measured by imaging the fiber ends onto a camera. The guiding power (0.5–4 mW) and the frequency were varied independently. The potential depth is approximately $U = \hbar\Omega^2/4|\delta|$ (far-detuned approximation), where Ω is the on-resonance Rabi frequency at the fiber center and δ is the detuning in radians per second from the center of the nearest transition. The spontaneous scattering rate is approximately $S = \Omega^2/4\tau\delta^2$. We use the convention $(\Omega\tau)^2 = I/I_{sat}$ where τ is the transition natural lifetime, I is the average light intensity, and I_{sat} is the effective multiline on-resonance saturation intensity for equally populated ground states without optical pumping (5.06×10^4 erg/cm^2 s for the $D2$ transition and 8.97×10^4 erg/cm^2 s for the $D1$ transition). Both the upper and lower measured cutoff speeds seem to scale roughly linearly with $\Omega/\sqrt{|\delta|}$ ($\propto\sqrt{U}$). From

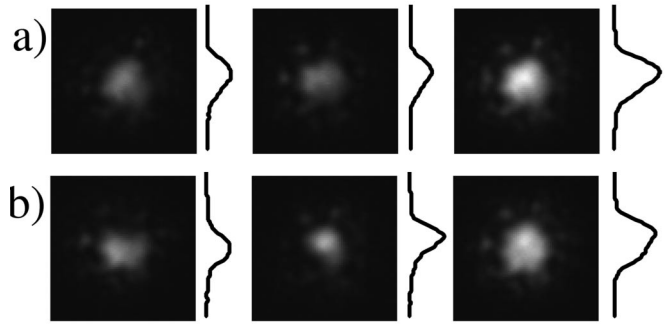

FIG. 2. Near-field HCPBG fiber mode images. (a) From left to right: horizontal, vertical, and crossed polarizations. (b) Same as in (a) but with all input polarizations rotated 45°.

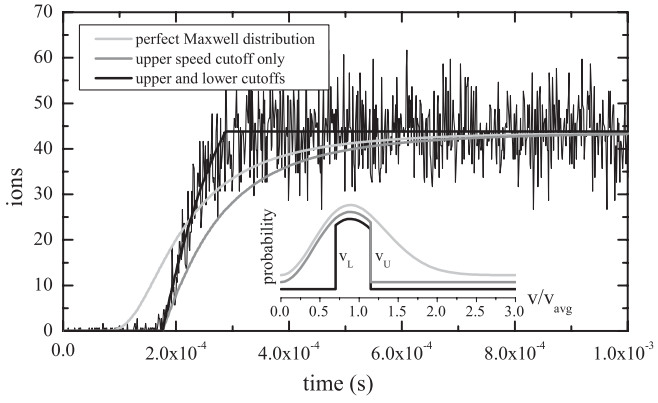

FIG. 3. Typical TOF spectrum (6.1 cm fiber). Slowing due to photon absorption is negligible in the models. Small delays for ion flight and AOM switching are included. The inset shows the model speed distributions versus speed—offset and scaled for comparison. The maximum input angle is assumed to be constant for all speeds.

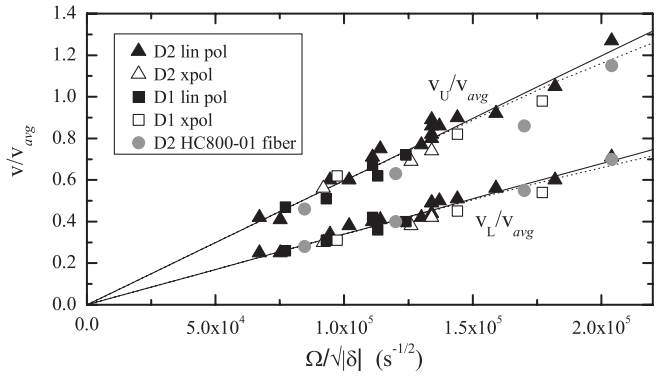

FIG. 4. Upper and lower cutoff speeds versus $\Omega/\sqrt{|\delta|}$ ($\approx\sqrt{4U/\hbar}$) for the 6.1 cm HC800-02 fiber. The solid lines are fits using the model $v = \sqrt{2U/m}/\theta$ with θ as a free parameter. The dotted lines use the actual potential depth instead of the far-detuned approximation. The open symbol data use two guiding beams with orthogonal polarizations (xpol). Uncertainty in the speeds is 10%.

a simple two-dimensional argument, we expect $v_U = \sqrt{2U/m}/\theta_{\max}$ where m is the atomic mass and $\theta_{\max}$ is the maximum angle of incidence. The linear fit shown in Fig. 4 implies an effective $\theta_{\max}$ of 10 mrad. This is close to the 8 mrad maximum angle of incidence allowed by the oven aperture. In a three-dimensional model, atoms with nonzero angular momentum with respect to the fiber axis can be guided at higher speeds and the effective angle should be smaller than 8 mrad. The discrepancy could exist because the upper cutoff is not sudden. Misalignment between the fiber and the nozzle, slight fiber curvature, and aging may also be important.

The lower cutoff has no obvious interpretation. Because the data depend only on potential depth, photon scattering cannot be responsible. A lower cutoff due to dipole force fluctuation heating should scale as $v_L \propto L\Omega^6/|\delta|^5$ [5]. Axial to transverse motion coupling due to roughness of the potential is unlikely to be the culprit because single-beam guiding, which has a more irregular potential, has the same cutoffs as two-beam guiding. To investigate the effect of the guiding light in the detection region, the distance between the fiber exit and the detection beams was varied from 0.1 to 1.2 cm, but had no effect on the cutoff speeds. The ion count rate showed complete saturation as a function of the detection pump and repump beam powers, even for the largest guiding laser Stark shifts. Because the lower cutoff is not constant, the data also rule out collisions with background gas as a mechanism. Increasing the background pressure by heating the fiber to 105 °C did not change the TOF signal. Assuming the background gas is H_2 diffusing through the fused silica fiber walls, we can calculate the average Rb-H_2 collision cross section [12] and set the upper limit on the background pressure inside the 6.1 cm fiber at 6×10^{-6} Torr.

One possible explanation for the lower cutoff velocity is wall collisions due to local loss of transverse confinement (caused by speckle). The transverse oscillation frequency ω_0 near the bottom of a Gaussian potential is proportional to $\sqrt{U}$. If the probability to survive a wall encounter is η, then for a fiber of length L the lower cutoff speed would scale roughly as $v_L \propto L\sqrt{U}\ln\eta$. To test this, we took TOF spectra of a shorter fiber (4.0 cm). The lower cutoff speeds remained the same, which rules out this mechanism (Fig. 5). The upper cutoffs for this fiber were much higher and were not proportional to $\sqrt{U}$. They decreased over several days. This is consistent with large signals we saw initially in the 6.1 cm fibers which decreased and stabilized by the time we took TOF data. This time dependence is currently not understood.

Another possible explanation for the lower cutoff is wall collisions in the optical coupling region where the atoms exit the fiber. The low coupling efficiency (10%–30%) suggests that the potential might be lower at the walls in this part of the fiber because the input beam spot is larger than the fiber mode and propagates a short distance into the fiber. Reducing the numerical aperture (NA) of the input light by a factor of 2.3 resulted in a slightly higher lower cutoff speed (Fig. 5). This is the qualitative result expected for wall collisions due to imperfect guiding light coupling.

We also investigated the fiber throughput as a function of guiding light power and detuning (Fig. 6). The ion count rate R and total throughput Q are given by

$$R = \epsilon\sqrt{\frac{2}{\pi}}\frac{nAN_E\sigma P\lambda}{w_B hc}\left[\frac{2}{\sqrt{\pi}}(\nu_L e^{-\nu_L^2} - \nu_U e^{-\nu_U^2}) + \mathrm{erfc}(\nu_L) - \mathrm{erfc}(\nu_U)\right], \quad (1)$$

$$Q = nAv_{\mathrm{avg}}[(\nu_L^2 + 1)e^{-\nu_L^2} - (\nu_U^2 + 1)e^{-\nu_U^2})], \quad (2)$$

where $\nu \equiv v\sqrt{m/2k_BT}$. Q is the number of atoms in a Maxwell distribution between the cutoff curves measured

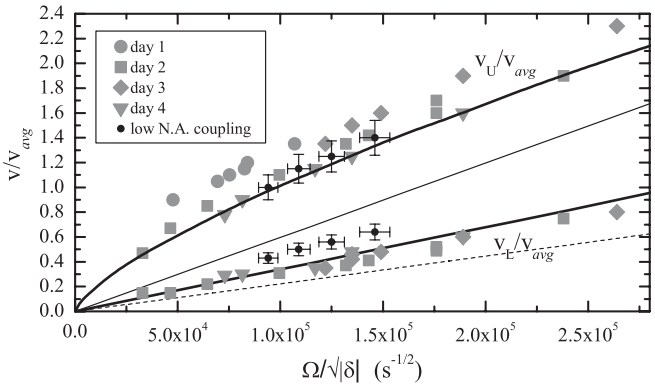

FIG. 5. Upper and lower cutoff speeds for the 4.0 cm HC800-02 fiber over several days. The two straight solid lines are from Fig. 4. The dotted line is the lower cutoff expected for scaling laws which are proportional to fiber length. The curved line is a power law fit to the day 4 upper cutoff data.

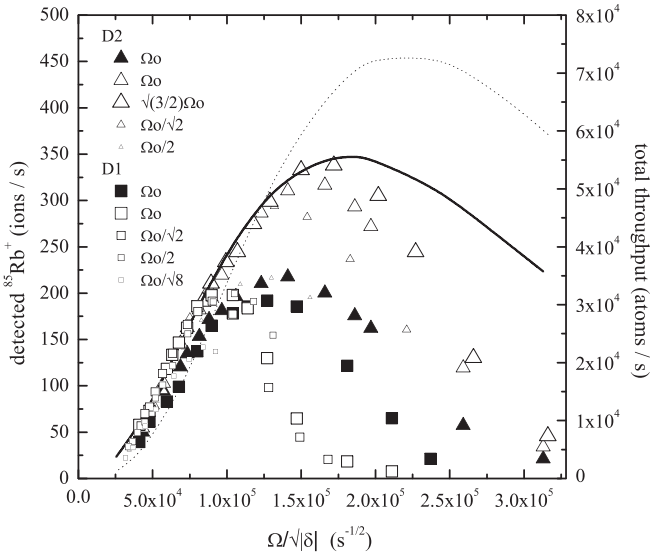

FIG. 6. Ions and total throughput for 4.0 cm fiber [16]. The guiding light detuning (δ) is swept for various values of the Rabi frequency (Ω). $\Omega o = 6.35 \times 10^{10}$ rad/s is an arbitrary Rabi frequency chosen for comparison. Open symbols are for two-beam guiding. Small $\Omega/\sqrt{|\delta|}$ is the low power, low scattering regime. Losses occur from spontaneous emission and perhaps desorption at large $\Omega/\sqrt{|\delta|}$. The solid curve is Eq. (1) multiplied by 1.05. The dotted curve is the throughput for both isotopes calculated from Eq. (2) and multiplied by 1.05.

in Fig. 5 which strike the effective capture area A of the fiber face (1.8×10^{-7} cm^2) per second. The density of the oven beam was measured by imaging the fluorescence of a resonant probe beam halfway between the nozzle and the fiber. The density at the fiber n is assumed to be a factor of 4 lower (1.1×10^7 cm^{-3} for ^{85}Rb). The $5P \rightarrow$ continuum beam has a power P (typically 0.7 W), a $1/e^2$ radius w_B (0.031 cm), and is smaller than the pump and repump beams. The calculated $5P$ photoionization cross section at $\lambda = 458$ nm is $\sigma = 1.3 \times 10^{-17}$ cm^2 [13]. The excited fraction in the $5P$ state N_E is $\frac{1}{2}$ and the Channeltron detection efficiency ϵ is assumed to be 0.85. When the curves are multiplied by 1.05 they fit the data well. Taking into account the 25% uncertainty in R (dominated by uncertainty in A) and the 10% uncertainty in the ion data, the guiding efficiency must be greater than 70%. This is in contrast with the slow-atom guide of Ref. [7], where multimode speckle causes local loss of confinement, and the estimated guiding efficiency is 3%. The thermal atom guide of Ref. [4] has an estimated guiding efficiency of over 40%. Rb atoms in our 4.0 cm guide undergo an average of 44 wall encounters. This is 1.5 times as many (9 times as many per centimeter) as in [7] and 5 times as many (4 times as many per centimeter) as in [4]. Our guide acts as a crude speed filter and the slowest atoms observed ($0.3v_{avg}$) are 9 times faster than the laser-cooled atoms in [7]. Our number of wall encounters per centimeter is constant because ω_0 and the average atom speed both scale roughly as $\sqrt{U}$. For a fixed potential depth, the counts decrease from the model limit as the spontaneous scattering rate increases (Ω decreases). This is likely due to dipole force fluctuation heating [5]. At large Ω, guiding is limited possibly through desorption of adsorbed Rb from the inner walls [9]. For high powers, the transmitted power decreases over 20 s or so to 2 mW at 780 nm (6 mW at 795 nm). This is possibly a thermal effect due to glass corroded by Rb, or a desorption effect [14].

Our data suggest that a slow-atom interferometer will need better light coupling to eliminate the low-speed cutoff. Input spot size is limited by our large working distance (8 cm) and thus large wave front distortion from the chamber window and optics, so intrachamber optics are likely to be needed. Short focal length aspheres can give coupling efficiencies of over 70%. Our transverse zero point temperatures are as large as 10 μK—within the range of optical molasses. The simplest interferometer to implement would be an accelerometer—a straight waveguide with Raman beams inside the fiber [15].

This work was supported by the National Science Foundation (Grant No. PHY0355202) and the Defense Advanced Research Projects Agency (Precision Inertial Navigation Systems grant).

[1] Y. J. Wang *et al.*, Phys. Rev. Lett. **94**, 090405 (2005).
[2] M. P. A. Jones *et al.*, Phys. Rev. Lett. **91**, 080401 (2003).
[3] C. Henkel and M. Wilkens, Europhys. Lett. **47**, 414 (1999).
[4] H. Ito *et al.*, Phys. Rev. Lett. **76**, 4500 (1996).
[5] M. J. Renn *et al.*, Phys. Rev. A **55**, 3684 (1997).
[6] R. G. Dall *et al.*, J. Opt. B **1**, 396 (1999).
[7] D. Müller *et al.*, Phys. Rev. A **61**, 033411 (2000).
[8] R. F. Cregan *et al.*, Science **285**, 1537 (1999).
[9] S. Ghosh *et al.*, Phys. Rev. Lett. **97**, 023603 (2006).
[10] The mode changes with a period of 340 GHz. No etalon effects were observed in the input light or the camera.
[11] M. Wegmüller *et al.*, Opt. Express **13**, 1457 (2005). At 860 nm, linearly polarized input light always gives a clean, roughly Gaussian mode.
[12] D. J. Croucher and J. L. Clark, J. Phys. B **2**, 603 (1969); H. L. Kramer and D. R. Herschbach, J. Chem. Phys. **53**, 2792 (1970); with van der Waals constants and polarizabilities from A. Derevianko, J. F. Babb, and A. Dalgarno, Phys. Rev. A **63**, 052704 (2001); E. Hult *et al.*, Phys. Rev. B **59**, 4708 (1999).
[13] T. Takekoshi *et al.*, Phys. Rev. A **69**, 053411 (2004). This is the $5P_{3/2} \rightarrow$ continuum cross section. Almost all of the excited atoms are in $5P_{3/2}$, as verified by trying 476 nm light instead of 458 nm light.
[14] This effect is not observed in fibers outside the chamber not exposed to Rb.
[15] M. Kasevich and S. Chu, Appl. Phys. B **54**, 321 (1992).
[16] Over the lifetime of the experiment, the oven flux decayed by a factor of 5. The 6.1 cm fiber had higher throughputs but the data were not self-consistent. This is because the data were taken earlier, and over a long span of time.